Bioorganic & Medicinal Chemistry Letters 24 (2014) 382–385

Contents lists available at ScienceDirect

Bioorganic & Medicinal Chemistry Letters

journal homepage: www.elsevier.com/locate/bmcl

Asymmetric synthesis and receptor activity of chiral simplified resiniferatoxin (sRTX) analogues as transient receptor potential vanilloid 1 (TRPV1) ligands

Myeong Seop Kim [a], Yooran Ki [a], Song Yeon Ahn [a], Suyoung Yoon [a], Sung-Eun Kim [a], Hyeung-Geun Park [a], Wei Sun [b], Karam Son [c], Minghua Cui [c], Sun Choi [c], Larry V. Pearce [d], Timothy E. Esch [d], Ian A. DeAndrea-Lazarus [d], Peter M. Blumberg [d], Jeewoo Lee [a,*]

[a] Research Institute of Pharmaceutical Sciences, College of Pharmacy, Seoul National University, Seoul 151-742, Republic of Korea
[b] Shenyang Pharmaceutical University, Shenyang, Liaoning 110016, China
[c] National Leading Research Lab of Molecular Modeling & Drug Design, College of Pharmacy, Graduate School of Pharmaceutical Sciences and Global Top 5 Research Program, Ewha Womans University, Seoul 120-750, Republic of Korea
[d] Laboratory of Cancer Biology and Genetics, Center for Cancer Research, National Cancer Institute, NIH, Bethesda, MD 20892, USA

ARTICLE INFO

Article history:
Received 25 September 2013
Revised 20 October 2013
Accepted 29 October 2013
Available online 6 November 2013

Keywords:
Vanilloid receptor 1
TRPV1 antagonist
Capsaicin
Resiniferatoxin
Molecular modeling

ABSTRACT

The chiral isomers of the two potent simplified RTX-based vanilloids, compounds **2** and **3**, were synthesized employing highly enantioselective PTC alkylation and evaluated as *h*TRPV1 ligands. The analysis indicated that the *R*-isomer was the eutomer in binding affinity and functional activity. The agonism of compound **2*R*** was comparable to that of RTX. Docking analysis of the chiral isomers of **3** suggested the basis for its stereospecific activity and the binding mode of **3*R***.

The transient receptor potential V1 (TRPV1) receptor[1] is a molecular integrator of nociceptive stimuli and functions as a non-selective cation channel with high Ca^{2+} permeability. The receptor is activated by protons,[2] heat,[3] endogenous inflammatory mediators[4,5] and natural vanilloids such as capsaicin (CAP)[6] and resiniferatoxin (RTX).[7] Its activation leads to an increase in intracellular Ca^{2+} that results in excitation of primary sensory neurons and ultimately the central perception of pain.

RTX has proven to function pharmacologically as an ultrapotent agonist for TRPV1, for example displaying 10^3- to to 10^4-fold greater potency than the prototypic agonist capsaicin.[8] In order to find a simple surrogate of RTX, we initially analyzed the pharmacophores of RTX based on previous SAR investigations and proposed a pharmacophoric model in which the principal pharmacophores were the 4-hydroxy-3-methoxyphenyl (A-region), C_{20}-ester (B-region), orthophenyl (C_1-region) and C_3-keto (C_2-region) groups.[9] On the basis of this model, we have extensively investigated simplified RTX surrogates embodying the principal pharmacophores of RTX to find potent agonists[9,10] as well as antagonists[11–13]

These extensive efforts identified the template of *N*-(3-acyloxy-2-benzylpropyl)-*N*′-benzyl thiourea as an optimized surrogate of RTX. Compounds **2** and **3** represent the prototypic agonist and antagonist with high affinity as simplified RTX-based vanilloids in the rat TRPV1/CHO system.[10,13] Their key pharmacophores are color-coded to show their correspondence with the pharmacophores of RTX (Fig. 1). Since the C-region of compounds **2** and **3**, viz. the 3-pivaloyl-2-(4-*t*-butylbenzyl)propyl group, has a chiral center, its active enantiomer is expected to make a stereospecific interaction with the receptor as previously observed in a series of propanamides.[12]

Here we describe the asymmetric syntheses and receptor activities of the chiral isomers of **2** and **3** as well as modeling analysis using our human TRPV1 homology model to explain the stereospecific activity of the compounds.

The A-region of compound **2** was synthesized from vanillin in 4 steps (Scheme 1). The hydroxyl of vanillin (**4**) was protected and the product then reduced to give alcohol **5**. The hydroxyl of **5** was converted to the azide with diphenylphosphoryl azide and then transformed to the corresponding isothiocyanate **6** using carbon disulfide and triphenyphosphine.[14] The A-region of compound **3** was prepared from commercially available **7** in 3 steps

* Corresponding author.
E-mail address: jeewoo@snu.ac.kr (J. Lee).

0960-894X/$ - see front matter © 2013 Elsevier Ltd. All rights reserved.
http://dx.doi.org/10.1016/j.bmcl.2013.10.064

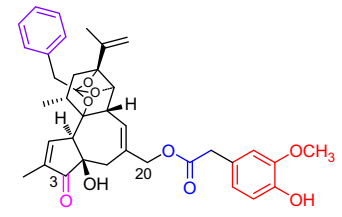

1 Resiniferatoxin (RTX)

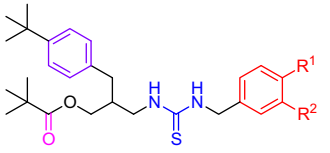

2 R^1=OH, R^2=OCH_3
3 R^1=$NHSO_2CH_3$, R^2=F

Figure 1. Resinifertoxin (RTX) and simplified RTX (sRTX).

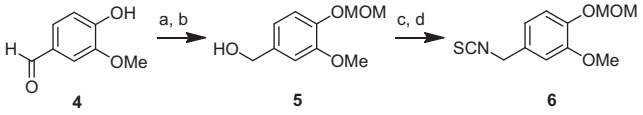

4 **5** **6**

Scheme 1. Synthesis of the A-region of compound **2**. Reagents and conditions: (a) DIEA, MOMCl, CH2Cl2, rt, 2 h, 99%; (b) NaBH4, LiCl, THF, EtOH, 0 °C, 1 h , 99%; (c) DPPA, DBU, toluene, rt, 1 h, 99%; (d) CS2, PPh3, THF, reflux, 2 h, 60%.

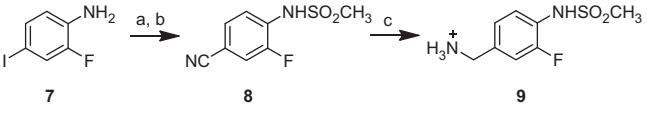

7 **8** **9**

Scheme 2. Synthesis of the A-region of compound **3**. Reagents and conditions: (a) MsCl, pyridine, rt, 2 h, 98%; (b) Zn(CN)2, Pd(PPh3)4, DMF, 150 °C, 15 h, 85%; (c) 2 M BH3-SMe2 in THF, reflux, 3 h then 1 M HCl, reflux, 15 h, 92%.

(Scheme 2). The amine of **7** was mesylated and then its iodide was converted into the corresponding nitrile to provide nitrile **8**, which was reduced to afford the amine **9**.

The asymmetric synthesis of the C-region utilized the highly enantioselective phase-transfer catalytic mono-alkylation of malonamic ester as a key step, previously reported by Park and Jew et al. (Schemes 3 and 4).[15] The substrate for asymmetric alkylation, *N*,*N*-bis(p-methoxyphenyl) malonamide *tert*-butyl ester (**11**), was prepared from malonic monoester **10**. The phase-transfer catalytic α-alkylation of **11** in the presence of (*R*,*R*)-3,4,5-trifluorophenyl-NAS bromide using 4-*t*-benzyl bromide afforded the highly enantioselective **12*R*** (99%, 92% ee). The $LiAlH_4$ reduction of **12*R*** produced the 3-aminopropanol **13*R***, whose di-PMP protecting group was converted into the corresponding Boc group to give **14*R***. The alcohol of **14*R*** was pivaloylated and then the *N*-Boc group was deprotected to yield the C-region amine **15*R***. Finally, the coupling of **15*R*** with isothiocyanate **6** followed by MOM-deprotection provided the final compound **2*R***. The amine of **15*R*** was converted to the corresponding isothiocyanate, which was coupled with amine **9** to provide the final **3*R***.

To prepare the corresponding ***S***-isomers, the phase-transfer catalytic α-alkylation of **11** employing (*S*,*S*)-ligand provided **12*S*** with high enantioselectivity (99%, 99% ee). With **12*S***, the same routes used in Scheme 3 produced the final **2*S*** and **3*S***, respectively. The structures and optical purities of final compounds were confirmed by spectroscopic data and chiral HPLC.[16]

The binding affinities and potencies as agonists/antagonists of the synthesized TRPV1 ligands were assessed in vitro by a binding competition assay with [^{3}H]RTX and by a functional $^{45}Ca^{2+}$ uptake assay using human TRPV1 heterologously expressed in Chinese hamster ovary (CHO) cells, as previously described.[17,18] The results are summarized in Table 1, together with the potencies of RTX, I-RTX and racemates **2** and **3**.

The receptor activities of compounds **2** and **3** were previously reported for the rat TRPV1/CHO system[10,13] and are reported here for human TRPV1 compared to the activities of RTX and I-RTX. Compound **2** proved to be a potent agonist for *h*TRPV1 with K_i = 6.1 nM and EC_{50} = 1.34 nM; it was thus within ca. 5- and 1.5-fold of the potency of RTX in binding affinity and agonism, respectively, with human TRPV1. Compound **3** was a potent *h*TRPV1 antagonist with K_i = 23 nM and $K_{i(ant)}$ = 122 nM, which was ca. 2- and 20-fold less potent than I-RTX in binding affinity and antagonism, respectively.

Analysis of the chiral isoforms indicated that the *R*-isomer was the more active isomer for both compounds **2** and **3**. In the case of

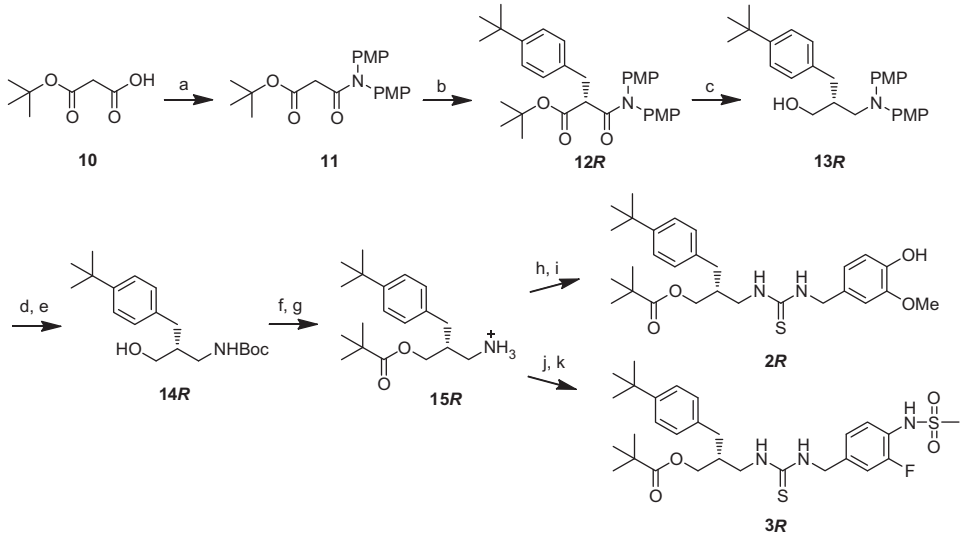

10 **11** **12*R*** **13*R*** **14*R*** **15*R*** **2*R*** **3*R***

Scheme 3. Syntheses of (*R*)-sRTX isomers Reagents and conditions: (a) 4,4′-dimethoxydiphenyl amine, EDC, DMAP, CH_2Cl_2, rt, 20 h, 98%; (b) (*R*,*R*)-3,4,5-trifluorophenyl-NAS bromide, 4-*t*-butylbenzyl bromide, 50% KOH, toluene, −40 °C, 24 h, 99%; (c) $LiAlH_4$, dibutyl ether, reflux, 1 h, 70%; (d) CAN, H_2O, CH_3CN, 0 °C, 30 min; (e) 8 N NaOH, Boc_2O, rt, 7 h, 60% for 2 steps; (f) $C(CH_3)_3COCl$, DMAP, CH_2Cl_2, rt, 4 h, 95%; (g) CF_3CO_2H, CH_2Cl_2, rt, 2 h; (h) compound **6**, NEt_3, CH_2Cl_2, rt, 20 h, 80% for 2 steps; (i) CF_3CO_2H, CH_2Cl_2, 0 °C, 1 h, 60%; (j) 1,1′-thiocarbonyldi-2-pyridone, NEt_3, DMF, rt, 15 h, 75% for 2 steps; (k) compound **9**, NEt_3, CH_2Cl_2, rt, 15 h, 70%.

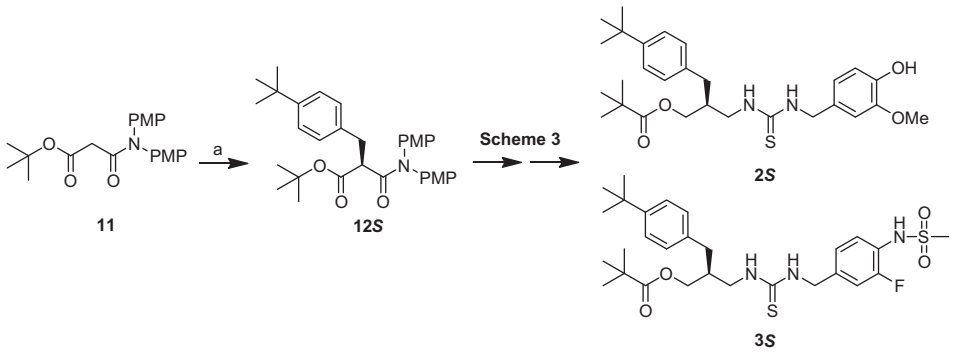

Scheme 4. Syntheses of (*S*)-sRTX isomers Reagents and conditions: (a) (*S*,*S*)-3,4,5-trifluorophenyl-NAS bromide, 4-*t*-butylbenzyl bromide, 50% KOH, toluene, −40 °C, 24 h, 99%.

Table 1
Binding affinities and functional activities to human TRPV1[a]

	Binding affinity K_i (nM)	Agonism (EC_{50}, nM)	Antagonism (K_i, nM)
RTX	1.23 (±0.22)	0.92 (±0.19)	NE
2	6.1 (±1.7)	1.34 (±0.27)	NE
2R	3.06 (±0.57)	0.99 (±0.10)	NE
2S	6.58 (±0.40)	9.55 (±0.41)	NE
I-RTX	11.8 (±3.1)	NE	5.9 (±1.3)
3	23.0 (±4.6)	NE	122 (±29)
3R	17.2 (±4.3)	NE	94 (±19)
3S	63 (±17)	NE	161 (±38)

[a] NE: not effective, mean ± SEM of at least three experiments.

the chiral isomers of **2**, eutomer ***2R*** yielded values for binding affinity and agonism of K_i = 3.06 nM and EC_{50} = 0.99 nM, which reflect 2- and 1.5-fold greater potency than was found for the racemate **2**. We conclude that ***2R*** was highly potent as an agonist for hTRPV1 and its potency was comparable to that of the superpotent RTX. Conversely, distomer ***2S*** was 1.1- and 7-fold less potent than **2** in affinity and agonism, respectively. In the case of the chiral isomers of **3**, the eutomer ***3R***, with values of K_i = 17.2 nM and $K_{i(ant)}$=94.4 nM, showed 1.3-fold greater potency than **3** both in binding affinity and antagonism; conversely, the distomer ***3S*** exhibited 3- and 1.3-fold less potency compared to **3** for binding affinity and antagonism, respectively.

Previously, we performed docking analysis of the sRTX agonist **2** using the rat TRPV1 homology model constructed independently and we demonstrated its binding mode compared to capsaicin and RTX.[19] In order to understand the stereospecific activities and binding modes of ***3R*** and ***3S***, we performed flexible docking studies using our human TRPV1 model[20] built based on our rat TRPV1 model.[19]

Analysis of energy minimization yielded calculated binding energies for ***3R*** and ***3S*** of −313.40 kcal/mol and −278.80 kcal/mol, respectively. The more favorable binding energy of ***3R*** than of ***3S*** was consistent with its stereospecific receptor activity. As illustrated in Figure 2, **3R** showed an excellent fit to the binding site with a different binding mode compared to previous propanamide antagonists.[20] The sulfonylaminobenzyl group (A-region) occupied the deep bottom hole and was involved in the hydrophobic interactions with Val508, Tyr511, Ile564, Tyr565, and Ile569. Furthermore, the NH of the sulfonamide group participated in

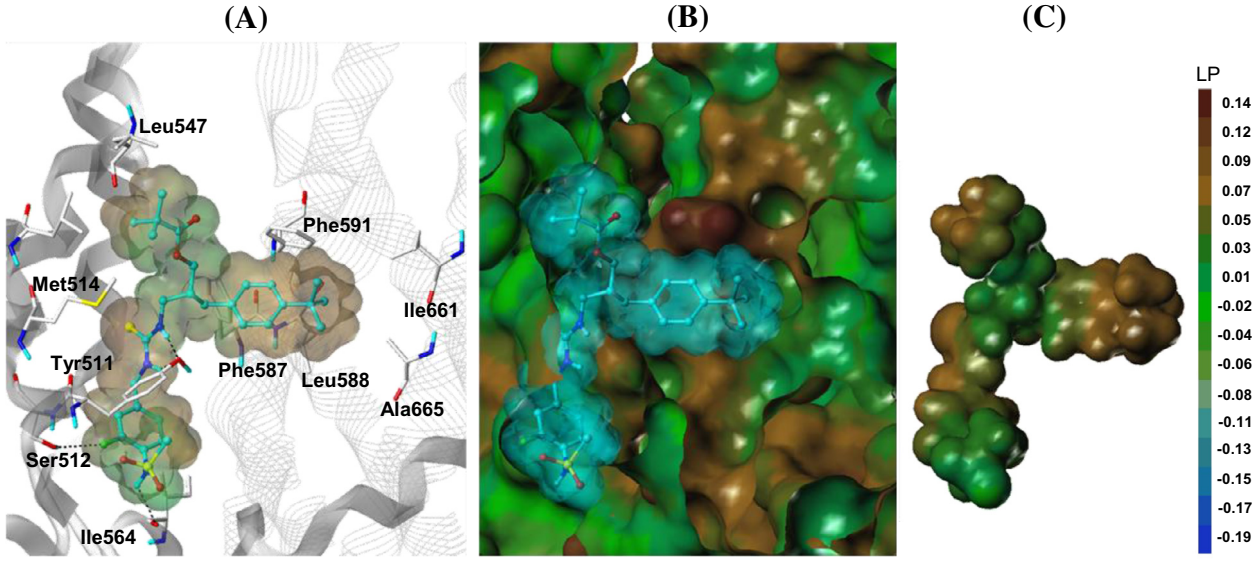

Figure 2. Flexible docking of ***3R*** in the *h*TRPV1 model. (A) Binding mode of ***3R***. The key residues are marked and displayed as capped-stick with carbon atoms in white. The ligand is depicted as ball-and-stick with carbon atoms in cyan. The Fast Connolly surface of *h*TRPV1 was generated by MOLCAD and colored by the lipophilic potential property. The surface of *h*TRPV1 is Z-clipped. The van der Waals surface of the ligand was presented with its carbon color for clarity. Hydrogen bonds are shown in black dashed lines and non-polor hydrogens are undisplayed for clarity. (C) Van der Waals surface of the ligand colored by its lipophilic potential property.

hydrogen bonding with Ile564, and the fluorine atom of the A-region made a hydrogen bond with Ser512. The thiourea group (B region) made a hydrogen bond with Tyr511 and also contributed to the appropriate positioning of the C-region for hydrophobic interactions. The Boc group in the C-region extended toward Met514, Leu518, and Leu547 in the hydrophobic area, and the 4-*t*-butylbenzyl group made tight interactions with the adjacent monomer's hydrophobic region, composed of Phe587, Leu588, Phe591, Ile661, and Ala665.

In summary, the chiral isomers of the two potent simplified RTX-based vanilloids, agonist **2** and antagonist **3**, were synthesized with high optical purity employing highly enantioselective PTC alkylation and evaluated as *h*TRPV1 ligands. The *R*-isomer of the 3-pivaloyloxy-2-(4-t-butylbenzyl)propyl C-region was the eutomer in binding affinity and functional activity, and the agonism of compound **2** for *h*TRPV1 was comparable to that of RTX. The docking analysis of the chiral isomers of **3** with our *h*TRPV1 homology model demonstrated the more favorable binding energy of the preferred isomer **3*R*** and its binding mode.

Acknowledgments

This research was supported by the National Research Foundation of Korea (NRF) Grant (2007-0056817) and NLRL program Grant (2011-0028885) funded by the Korea government MSIP, and was supported in part by the Intramural Research Program of the National Institutes of Health, Center for Cancer Research, National Cancer Institute (Project Z1A BC 005270).

References and notes

1. Szallasi, A.; Blumberg, P. M. *Pharmacol. Rev.* **1999**, *51*, 159.
2. Tominaga, M.; Caterina, M. J.; Malmberg, A. B.; Rosen, T. A.; Gilbert, H.; Skinner, K.; Raumann, B. E.; Basbaum, A. I.; Julius, D. *Neuron* **1998**, *21*, 531.
3. Caterina, M. J.; Schumacher, M. A.; Tominaga, M.; Rosen, T. A.; Levine, J. D.; Julius, D. *Nature* **1997**, *389*, 816.
4. Zygmunt, P. M.; Petersson, J.; Andersson, D. A.; Chuang, H.-H.; Sorgard, M.; Di Marzo, V.; Julius, D.; Hogestatt, E. D. *Nature* **1999**, *400*, 452.
5. Hwang, S. W.; Cho, H.; Kwak, J.; Lee, S. Y.; Kang, C. J.; Jung, J.; Cho, S.; Min, K. H.; Suh, Y. G.; Kim, D.; Oh, U. *Proc. Natl. Acad. Sci. U.S.A.* **2000**, *97*, 6155.
6. Walpole, C. S. J.; Wrigglesworth, R. *Capsaicin in the Study of Pain*; Academic Press: San Diego, CA, 1993; p 63.
7. Appendino, G.; Szallasi, A. *Life Sci.* **1997**, *60*, 681.
8. Szallasi, A.; Blumberg, P. M. *Neuroscience* **1989**, *30*, 515.
9. Lee, J.; Lee, J.; Kim, J.; Kim, S. Y.; Chun, M. W.; Cho, H.; Hwang, S. W.; Oh, U.; Park, Y. H.; Marquez, V. E.; Beheshti, M.; Szabo, T.; Blumberg, P. M. *Bioorg. Med. Chem.* **2001**, *9*, 19.
10. Lee, J.; Kim, S. Y.; Park, S.; Lim, J.-O.; Kim, J.-M.; Kang, M.; Lee, Ji.; Kang, S.-U.; Choi, H.-K.; Jin, M.-K.; Welter, J. D.; Szabo, T.; Tran, R.; Pearce, L. V.; Toth, A.; Blumberg, P. M. *Bioorg. Med. Chem.* **2004**, *12*, 1055.
11. Lee, J.; Lee, J.; Kang, M.; Shin, M.-Y.; Kim, J.-M.; Kang, S.-U.; Lim, J.-O.; Choi, H.-K.; Suh, Y.-G.; Park, H.-G.; Oh, U.; Kim, H.-D.; Park, Y.-H.; Ha, H.-J.; Kim, Y.-H.; Toth, A.; Wang, Y.; Tran, R.; Pearce, L. V.; Lundberg, D. J.; Blumberg, P. M. *J. Med. Chem.* **2003**, *46*, 3116.
12. Ryu, H.; Jin, M.-K.; Kang, S.-U.; Kim, S. Y.; Kang, D. W.; Lee, J.; Pearce, L. V.; Pavlyukovets, V. A.; Morgan, M. A.; Tran, R.; Toth, A.; Lundberg, D. J.; Blumberg, P. M. *J. Med. Chem.* **2008**, *51*, 57.
13. Bhondwe, R. S.; Kang, D. W.; Kim, M. S.; Kim, H. S.; Park, S.-G.; Son, K.; Choi, S.; Lang Kuhs, K. A.; Pavlyukovets, V. A.; Pearce, L. V.; Blumberg, P. M.; Lee, J. *Bioorg. Med. Chem. Lett.* **2012**, *22*, 3656.
14. Isoda, T.; Hayashi, K.; Tamai, S.; Kumagai, T.; Nagao, Y. *Chem. Pharm. Bull.* **2006**, *54*, 1616.
15. Kim, M.-H.; Choi, S.-H.; Lee, Y.-J.; Lee, J.; Nahm, K.; Jeong, B.-S.; Park, H.-G.; Jew, S.-S. *Chem. Commun.* **2009**, 782.
16. *Compound* **2*R***: white solid. mp 60–73 °C, α_D^{20} −3.53 (*c* 0.8, $CHCl_3$), ^{1}H NMR (400 MHz, $CDCl_3$) δ 7.27 (d, *J* = 8.24 Hz, 2H), 7.07 (d, *J* = 8.12 Hz, 2H), 6.83 (t, 2H), 6.77 (d, 1H), 6.22 (br t, 1H), 6.02 (br s, 1H), 5.60 (br s, 1H), 4.37 (br s, 2H), 4.12 (dd, *J* = 11.52, 3.84 Hz, 1H), 3.84 (s, 3H), 3.78 (dd, *J* = 11.48, 4.64 Hz, 1H), 3.72 (br s, 1H), 3.24 (pentet, 1H), 2.56 (qd, 2H), 2.28 (m ,1H), 1.26 (s, 9H), 1.19 (s, 9H). MS (FAB) *m*/*z* 501 (MH^+), HRMS calcd for $C_{28}H_{40}N_2O_4S$ (M+H), 501.2786, found 501.2774. Optical purity: ee 96% (Daicel Chiralcel OD-H, Retention time = 30 min, Eluent: n-Hep:IPA = 9:1.
Compound **2*S***: white solid, mp 64–74 °C, α_D^{20} + 5.85 (*c* 0.8, $CHCl_3$), ^{1}H NMR (400 MHz, $CDCl_3$) δ 7.27 (d, *J* = 8.24 Hz, 2H), 7.07 (d, *J* = 8.12 Hz, 2H), 6.84 (t, 2H), 6.77 (d, 1H), 6.20 (br t, 1H), 5.97 (br s, 1H), 5.58 (br s, 1H), 4.37 (br s, 2H), 4.13 (dd, *J* = 11.52, 3.88 Hz, 1H), 3.85 (s, 3H), 3.78 (dd, *J* = 11.48, 4.64 Hz, 1H), 3.72 (br s, 1H), 3.24 (pentet, 1H), 2.55 (qd, 2H), 2.28 (m ,1H), 1.26 (s, 9H), 1.20 (s, 9H). MS (FAB) *m*/*z* 501 (MH^+), HRMS calcd for $C_{28}H_{40}N_2O_4S$ (M+H), 501.2787, found 501.2774. Optical purity: ee 97 % (Daicel Chiralcel OD-H, Retention time = 34 min, Eluent: n-Hep:IPA=9:1.
Compound **3*R***: white solid, mp 79-88 °C, α_D^{20} −9.4 (*c* 1.0, $CHCl_3$). ^{1}H NMR (500 MHz, $CDCl_3$) δ 7.47 (t, *J* = 8.2 Hz, 1H), 7.28 (d, *J* = 8.2 Hz, 2H), 7.12 (dd, *J* = 11 Hz, 1H), 7.08 (t, 3H), 6.62 (s, 1H), 6.41 (br t, 1H), 6.17 (br s, 1H), 4.57 (s, 2H), 4.15 (dd, *J* = 11.5, 3.75 Hz, 1H), 3.81 (d, *J* = 7.7 Hz, 1H), 3.72 (s, 1H), 3.18 (m, 1H), 2.98 (s, 3H), 2.58 (qd, 2H), 2.30 (m, 1H), 1.26 (s, 9H), 1.20 (s, 9H). MS (FAB) *m*/*z* 566 (MH^+), HRMS calcd for $C_{28}H_{40}FN_3O_4S_2$ (M+H), 566.2523, found 566.2512. Optical purity: ee 95% (Daicel Chiralpak IA, Retention time = 18.1 min, Eluent: n-Hex:EtOH=9:1).
Compound **3*S***: white solid, mp 77–88 °C, α_D^{20} 7.524 (*c* 1.0, $CHCl_3$). ^{1}H NMR (500 MHz, $CDCl_3$) δ 7.48 (t, *J* = 8.15 Hz, 1H), 7.28 (d, *J* = 8.15 Hz, 2H), 7.12 (dd, *J* = 11, 1.3 Hz, 1H), 7.08 (t, 3H), 6.59 (s, 1H), 6.39 (br t, 1H), 6.13 (br s, 1H), 4.57 (s, 2H), 4.16 (dd, *J* = 11.5, 3.75 Hz, 1H), 3.80 (d, *J* = 7.7 Hz, 1H), 3.72 (s, 1H), 3.18 (m, 1H), 2.98 (s, 3H), 2.58 (qd, 2H), 2.30 (m, 1H), 1.26 (s, 9H), 1.20 (s, 9H).
MS (FAB) *m*/*z* 566 (MH^+), HRMS calcd for $C_{28}H_{40}FN_3O_4S_2$ (M+H), 566.2522, found 566.2512. Optical purity: ee 97% (Daicel Chiralpak IA, Retention time = 19.9 min, Eluent: n-Hex:EtOH = 9:1).
17. Min, K. H.; Suh, Y.-G.; Park, M.-K.; Park, H.-G.; Park, Y.-H.; Kim, H.-D.; Oh, U.; Blumberg, P. M.; Lee, J. [published erratum appears in *Mol. Pharmacol.* **2003**, *63*, 958] *Mol. Pharmacol.* **2002**, *62*, 947.
18. Veghel, D. V.; Cleynhens, J.; Pearce, L. V.; Blumberg, P. M.; Laere, K. V.; Verbruggen, A.; Bormans, G. *Nucl. Med. Bio.* **2013**, *40*, 141.
19. Lee, J. H.; Lee, Y.; Ryu, H.; Kang, D. W.; Lee, J.; Lazar, J.; Pearce, L. V.; Pavlyukovets, V. A.; Blumberg, P. M.; Choi, S. *J. Comput. Aided Mol. Des.* **2011**, *25*, 317.
20. Kim, M. S.; Ryu, H.; Kang, D. W.; Cho, S. H.; Seo, S.; Park, Y. S.; Kim, M. Y.; Kwak, E. J.; Kim, Y. S.; Bhondwe, R. S.; Kim, H. S.; Park, S. G.; Son, K.; Choi, S.; DeAndrea-Lazarus, I. A.; Pearce, L. V.; Blumberg, P. M.; Frank, R.; Bahrenberg, G.; Stockhausen, H.; Kögel, B. Y.; Schiene, K.; Christoph, T.; Lee, J. *J. Med. Chem.* **2012**, *55*, 8392.